

Research Paper

Ultrasonographic Imaging and Anti-inflammatory Therapy of Muscle and Tendon Injuries Using Polymer Nanoparticles

Gi-Wook Kim^{1, 2, 4*}, Changsun Kang^{3*}, Young-Bin Oh^{1, 2}, Myoung-Hwan Ko^{1, 2, 4}, Jeong-Hwan Seo^{1, 2, 4}, Dongwon Lee^{3, 5}

1. Department of Physical Medicine and Rehabilitation, Chonbuk National University Medical School, Chonbuk, 561-756, Republic of Korea;
2. Research Institute of Clinical Medicine of Chonbuk National University- Biomedical Research Institute of Chonbuk National University Hospital, Chonbuk, 561-756, Republic of Korea;
3. Department of BIN Convergence Technology, Chonbuk National University, Chonbuk, 561-756, Republic of Korea;
4. Translational Research & Clinical Trial Center for Medical Device, Chonbuk National University Hospital, Chonbuk, 561-756, Republic of Korea;
5. Department of Polymer-Nano Science and Technology, Chonbuk National University, Chonbuk, 561-756, Republic of Korea.

* These authors contributed equally to this work.

✉ Corresponding authors: Jeong-Hwan Seo, M.D., Ph.D. Phone: 82-63-250-1797, E-mail: vivaseo@jbnu.ac.kr, Fax: 82-63-254-4145 Dongwon Lee, Ph.D. Phone: 82-63-270-2344, E-mail: dlee@chonbuk.ac.kr, Fax: 82-63-270-2341

© Ivyspring International Publisher. This is an open access article distributed under the terms of the Creative Commons Attribution (CC BY-NC) license (<https://creativecommons.org/licenses/by-nc/4.0/>). See <http://ivyspring.com/terms> for full terms and conditions.

Received: 2016.12.26; Accepted: 2017.04.17; Published: 2017.06.24

Abstract

Ultrasonography is a reliable diagnostic modality for muscle and tendon injuries, but it has been challenging to find right diagnosis of minor musculoskeletal injuries by conventional ultrasonographic imaging. A large amount of hydrogen peroxide (H_2O_2) are known to be generated during tissue damages such as mechanical injury and therefore H_2O_2 holds great potential as a diagnostic and therapeutic marker for mechanical injuries in the musculoskeletal system. We previously developed poly(vanillyl alcohol-co-oxalate) (PVAX), which rapidly scavenges H_2O_2 and exerts antioxidant and anti-inflammatory activity in H_2O_2 -associated diseases. Based on the notion that PVAX nanoparticles generate CO_2 bubbles through H_2O_2 -triggered hydrolysis, we postulated that PVAX nanoparticles could serve as ultrasonographic contrast agents and therapeutic agents for musculoskeletal injuries associated with overproduction of H_2O_2 . In the agarose gel phantom study, PVAX nanoparticles continuously generated CO_2 bubbles to enhance ultrasonographic echogenicity significantly. Contusion injury significantly elevated the level of H_2O_2 in skeletal muscles and Achilles tendons. Upon intramuscular injection, PVAX nanoparticles significantly elevated the ultrasound contrast and suppressed inflammation and apoptosis in the contusion injury of musculoskeletal systems. We anticipate that PVAX nanoparticles hold great translational potential as theranostic agents for musculoskeletal injuries.

Key words: Ultrasonography, Musculoskeletal injury, Polymer nanoparticles, Hydrogen peroxide, CO_2 Bubbles.

Introduction

Musculoskeletal systems are commonly injured by direct contusion, immoderate exercise and muscle or ligament ruptures [1-2]. Muscle and tendon diseases frequently accompany degenerative changes [3-4]. Ultrasonography has been considered an important diagnostic tool alongside MRI (magnetic resonance imaging) for imaging the musculoskeletal system and diagnosing pathological conditions. In conventional ultrasonography, local hypoechoic areas

or indistinct fibrillar patterns characterize muscle and ligament injuries [5-6]. Ultrasonography using a high frequency transducer allows visualization of soft tissues and superficial structures with resolution approaching 200 μm , better than MRI [7]. However, mild injuries and small lesions are not easily detected with ultrasonography. Nevertheless, ultrasonography has been widely used for diagnosing the musculoskeletal injuries and applications of

musculoskeletal ultrasound have broadened due to its short imaging time, high resolution, capability for real-time dynamic imaging in comparison with the contralateral side and ultrasound-guided musculoskeletal interventions, which provide advantages over MRI [8-9].

Ultrasonographic contrast agents have been widely utilized in the clinical settings to improve the visibility of internal body structures and pathological conditions. Conventional ultrasound contrast agents are gas-filled microbubbles, which consist of inert perfluorocarbon gas sequestered by stabilizing shells such as lipids and proteins [10]. Microbubbles have a typical diameter of 1~8 μm and enhance the ultrasonographic signal intensity by resonance under the acoustic field because of their compressibility and deformability [11]. However, the applications of gas-filled microbubbles have been hampered by several drawbacks. Microbubble contrast agents are limited to microcirculation or vascularity and abdominal regions including liver, pancreas and kidney [12]. Microbubbles are also unable to extravasate to reach muscle and tendon injuries because of poor tissue penetration [13-15]. Moreover, microbubbles have insufficient stability because perfluorocarbon gas expands at body temperature and diffuses away through the defects of stabilizing shells [16]. Therefore, great efforts have been devoted to the development of new ultrasound contrast agents, which are able to penetrate tissues and have a long half-life in physiological environments to provide long-lasting contrast in ultrasonography.

Recently, stimulus-triggered gas-generating particles have emerged as a new strategy to achieve maximal diagnostic efficacy of ultrasonography. These particles were designed to continuously generate CO_2 bubbles from the degradation of carbonate linkages, CaCO_3 or NH_4CO_3 , allowing for the persistence of ultrasonographic imaging with strong echogenicity [16-19]. These gas-generating solid particles could permeate into host tumoral environments by tissue extravasation and exhibit strong ultrasonographic echogenicity by continuously producing CO_2 bubbles. In particular, CO_2 bubble-generating polycarbonate nanoparticles exhibited a significantly longer imaging time than a commercial ultrasound contrast agent SonoVue and provided more anatomic landmarks in ultrasonographic imaging. In this context, there have been great efforts for the development of bubble-generating particles as ultrasound contrast agents [20].

Reactive oxygen species (ROS) are known to be produced by trauma (e.g., crush injury, contusion, laceration, mechanical injury, etc.), tendinopathy,

delayed myalgia and muscular contraction [21-24]. Among various ROS, H_2O_2 is considered the most abundant due to its stability [25-26]. We previously reported that H_2O_2 -responsive poly(vanillyl alcohol-co-oxalate) (PVAX), which undergoes H_2O_2 -triggered degradation to exert antioxidant, anti-inflammatory and anti-apoptotic activities [27-28]. In our previous studies using mouse models of ischemia/reperfusion injury and acute liver failure, PVAX nanoparticles suppressed oxidative stress and displayed highly potent therapeutic actions by scavenging excessive H_2O_2 and releasing bioactive vanillyl alcohol. In chemical term, PVAX possesses peroxalate esters in its backbone, which react specifically with H_2O_2 to generate CO_2 .

Inspired by the promising echogenic nature of CO_2 bubbles in the previous studies, we hypothesized that PVAX nanoparticles generate CO_2 bubbles through H_2O_2 -mediated degradation and provide enhanced echogenicity for ultrasonographic imaging. We also hypothesized that PVAX nanoparticles could exert beneficial therapeutic effects in muscle and tendon injuries associated with overproduction of H_2O_2 . Here, we sought to establish whether PVAX nanoparticles have potential as ultrasonographic contrast agents as well as therapeutic agents for musculoskeletal injury using a rat model of musculoskeletal contusion injury.

Materials and Methods

Preparation of PVAX nanoparticles

PVAX was synthesized as previously reported [29]. In brief, 1,4-cyclohexanedimethanol (21.96 mmol), and 4-hydroxy-3-methoxy benzyl alcohol (5.49 mmol) were completely dissolved in 20 mL of tetrahydrofuran (THF) under nitrogen atmosphere, into which trimethylamine (60 mmol) was added. Oxalyl chloride (27.45 mmol) dissolved in 25 mL of THF was added to the mixed solution. Polymerization was allowed to continue for 6 h at room temperature. The obtained polymer was then extracted using dichloromethane (DCM) and then precipitated in cold hexane. The chemical structure of PVAX was confirmed by ^1H NMR in deuterated chloroform on a 400 MHz spectrometer: 7.0 ~ 7.3 (*m*, 3H, Ar), 5.3 (*m*, 2H $\text{OCH}_2\text{-PhO-CH}_3$), 4.1 ~ 4.2 (*m*, 4H, COOCH_2CH), 3.8 (*m*, 3H, OCH_3). The molecular weight of PVAX was determined to be ~12,000 Da with polydispersity of 1.6 by gel permeation chromatography. To generate the PVAX nanoparticles, 50 mg of PVAX polymer dissolved in 500 μL of DCM was added to 5 mL of 10% poly(vinyl alcohol) (PVA). The mixed solution was sonicated using a sonicator (Sonic Dismembrator 500, Fisher Scientific) for 30 seconds and then

homogenized using a homogenizer (PRO Scientific, PRO 2000) for 20 seconds to yield fine emulsion. The emulsion was further homogenized with a 1% PVA solution for 1 min. Solvent was eliminated by a rotary evaporator. PVAX nanoparticles were obtained after centrifugation at $11,000\times g$ at $4^{\circ}C$ for 5 min, and lyophilization. The size of the PVAX nanoparticles was measured using a particle size analyzer (Brookhaven Instrument Corp., Holtville, NY) based on dynamic light scattering (DLS) and their size and morphology were observed using a scanning electron microscope (SUPRA 40VP, Carl Zeiss, Germany).

Cytotoxicity assay of PVAX nanoparticles

MTT

(3-(4,5-dimethylthiazol-2-yl)-2,5-diphenyltetrazolium bromide) assay was performed to study the cytotoxicity of PVAX nanoparticles. Mouse macrophage RAW 264.7 cells (1×10^6 cells/well in a 24 well plate) were cultured in 1 mL of culture medium and were treated with various amounts of PVAX nanoparticles for 24 h. Each well was given 20 μ L of MTT solution and were incubated for 4 h. The resulting formazan crystals were dissolved by adding 200 μ L of dimethyl sulfoxide (DMSO). After 30 min of incubation, the absorbance at 570 nm was measured using a microplate reader (Biotek Instruments, Winooski, VT). The cell viability was obtained by comparing the absorbance of nanoparticles-treated cells to that of control cells.

Ultrasonographic imaging of PVAX nanoparticles

An ultrasonographic imaging instrument (Zone Ultra, Zonare Medical Systems, San Francisco, CA, USA) was used with a linear transducer with 5 to 14 MHz. Dimension of the probe was 62×10 mm and the viewing width was 55 mm. The ultrasonographic images were obtained from a long axis view by a physician with an extensive experience in musculoskeletal ultrasonography. For *in vitro* ultrasonographic imaging of PVAX nanoparticles, hand-made agar gel phantom was used to simulate body conditions. One hundred microliter of PVAX nanoparticles (1 mg/mL in phosphate buffer saline, PBS) was placed in the well of phantom gels with or without H_2O_2 . Ultrasonographic imaging (B-mode) was collected as a function of time. For comparison purposes, SonoVue was used as a control at a concentration of 5 mg/mL.

Determination of CO_2 generated from PVAX nanoparticles

PVAX nanoparticles (100 mg) were added into 5

mL of H_2O_2 solution (10 mM) in a vial capped with a septum. A syringe needle was inserted into the vial to take the air containing CO_2 at appropriate time intervals and the level of CO_2 was measured using gas chromatography (6890N GC, Agilent Technologies, Wilmington, DE, USA). The amount of CO_2 (I) was determined by measuring the area under the curve (AUC) of GC spectrum and the CO_2 generation was quantified by comparing with the amount of CO_2 generated from fully degraded PVAX nanoparticles (I_{max}).

A rat model of contusion injury

Sprague Dawley rats (8-week-old males, Orient BioTM, Korea) were anaesthetized with the intraperitoneal injection of ketamine mixed with xylazine (RompunTM) in the proportion of 8 to 1. In the lateral decubitus position, the hind limb of rats was fixed with the knee extended and the ankle dorsiflexed. Contusion injuries were induced using a compression instrument (TMS-PRO[®], FTC Corp., Sterling, VA, USA). The triceps surae muscle and the Achilles tendon of the hind limb were compressed using a flat probe (3 mm diameter) at the force of 160 N and the velocity of 20 mm/min, until it acquired the thickness of 0.5 mm. In the case of triceps surae muscles, contusion injury was induced to the region 1 cm proximal to the musculotendinous junction. In case of Achilles tendon contusion, contusion injury was induced to the region just proximal to calcaneus, namely, the Achilles tendon insertion. The injuries were marked with a Devon skin marker for ultrasound imaging and biopsies. PVAX nanoparticles were suspended with injectable normal saline at a concentration of 1 mg/mL and 300 μ L of suspension was directly injected into the musculotendinous junction between the triceps surae muscles and the Achilles tendon. For comparison purposes, SonoVue (300 μ L of 5 mg/mL) was directly injected into muscles and Achilles tendon. After the ultrasonographic imaging, the skin of the injured areas was sutured for recovery and further analysis. All animal experiments were approved by the Institutional Animal Care and Use Committee (IACUC) of Chonbuk National University (CBNU2015-084) and conducted in accordance with the regulation.

Determination of the level of H_2O_2 in the site of contusion injury

Contusion injury was induced in the triceps surae muscle and the Achilles tendon. The tissues of the triceps surae muscles and Achilles tendons were excised 6 h after the injury and lysed in PBS at a concentration of 10 mg/mL using a homogenizer.

Tissue lysates were centrifuged at 8,000×g for 10 min and the supernatants were carefully taken. The level of H₂O₂ in the supernatant was determined using the Amplex red assay kit (Invitrogen, Carlsbad, CA, USA) and a microplate reader (Biotek Instruments, Winooski, VT, USA). Fluorescent intensity (FI) of the injured tissues was compared with those of non-injured tissues.

Real-time polymerase chain reaction (RT-PCR)

PVAX nanoparticles were injected into the injured right limb 1 h after the induction of injury and left limbs served as control. The tissues of the injured areas were excised at 3 days after injection (n=6). Tissues were homogenized using TRIzol reagent (Life Technologies, Gaithersburg, MD, USA) and total RNA was extracted from the tissue according to the manufacturer's suggested protocol. RNA was precipitated with isopropanol and dissolved in diethylpyrocarbonate-treated distilled water. Total RNA (2 µg) was treated with RNase-free DNase (Invitrogen) and first-strand cDNA was made using a random hexamer primer provided in the first-strand cDNA synthesis kit (Applied Biosystems, Foster City, CA, USA). Glyceraldehyde-3-phosphate dehydrogenase (GAPDH) was used as a control. The PCR reaction was carried out in 384-well plates using the ABI Prism 7900HT Sequence Detection System (Applied Biosystems, Foster, CA, USA).

Western blot analysis

The tissues of the injured areas were excised at 3 days after injection of PVAX nanoparticles (n=6). After being washed with an ice-cold phosphate buffer, tissues were homogenized and lysed using the mammalian protein extraction reagent (M-PER, Pierce Biotechnology, Rockford, IL, USA) for 20 min on ice. After centrifugation at 10,000×g, pellets were lysed with a RIPA lysis buffer (150 mM NaCl, 50 mM Tris-HCl pH 8.0, 1% NP-40, 0.5% sodium deoxycholate, 0.1% sodium dodecyl sulfate) containing protease and phosphatase inhibitors. The homogenates containing 20 µg of protein were separated by sodium dodecylsulfate-polyacrylamide gel electrophoresis with 10 % resolving and 3 % acrylamide stacking gels and then transferred to nitrocellulose sheets. The blots were probed with 2 µg/mL of primary antibodies for Bcl-2, caspase-3, β-actin (Santa Biotechnology, Santa Cruz, CA, USA), and Bax (Cell signalings, Danvers, MA, USA) in the cold room. Horseradish peroxidase-conjugated IgG (Zymed, South San Francisco, CA, USA) was used as a secondary antibody to quantify protein expression. Immunocross reactivity of the proteins was visualized

using a Luminescent image analyzer (LAS-1000, Fujifilm, Japan).

Histological examination

The therapeutic effects of PVAX were evaluated by histological examination of the muscle and tendon tissues. Tissues were excised at 3 days after injection of PVAX nanoparticles and immediately fixed in a 4% formaldehyde solution. The fixed tissues were embedded in paraffin and sliced longitudinally into sections with thickness of 4 µm. The sections were mounted on glass slides and stained with hematoxylin and eosin (H&E) and TUNEL (Terminal deoxynucleotidyl transferase dUTP nick end labeling). The slides of the muscles and tendons were analyzed by a pathologist.

Statistical analysis

The statistical analyses were performed using SPSS (Version 18.0). Injured muscles and tendons were compared with the non-injured counterpart using the independent t-test in the Amplex red assay. Quantification in RT-PCR and western blot assay was performed using ImageJ and the one-way ANOVA with Scheffe method as post hoc test. The *p*-values less than 0.05 were considered statistically significant.

Results

Physicochemical properties of PVAX nanoparticles

PVAX was designed to degrade in a H₂O₂-triggered manner to generate vanillyl alcohol and CO₂ (Figure 1A and B). PVAX nanoparticles formulated by a conventional single emulsion were round spheres with smooth surface, confirmed by scanning electron microscopy. The hydrodynamic diameter of PVAX nanoparticles suspended in PBS was determined to be ~400 nm (Figure 1C). We first performed gas chromatography to verify the ability of PVAX nanoparticles to generate CO₂ in a H₂O₂-triggered manner. Figure 1D shows the quantification and generation kinetics of CO₂ from PVAX nanoparticles. The basal level of CO₂ was detected in the suspension of PVAX nanoparticles in PBS before the addition of H₂O₂. After the addition of H₂O₂, the level of CO₂ rapidly and gradually increased, demonstrating that CO₂ is continuously generated from the H₂O₂-triggered oxidation of peroxalate esters in the backbone of PVAX. At 40 min after the addition of H₂O₂, all peroxalate esters in the backbone of PVAX seemed to degrade and no further CO₂ generation was detected thereafter.

To investigate the hydrolysis mechanism and predict the CO₂ bubble generation, variations in the

hydrodynamic diameter and structure of PVAX nanoparticles were observed during incubation in PBS with or without H_2O_2 by DLS and transmission electron microscopy (TEM). In the absence of H_2O_2 , PVAX nanoparticles displayed slight increment in their size with monomodal distribution, implying that PVAX nanoparticles slightly swelled without significant changes in structural robustness (Figure 1E and F). However, in the presence of H_2O_2 (100 μM), PVAX nanoparticles displayed a significantly increased diameter, with broad distribution ranging from 1 to 3 μm . Small fractions at ~ 200 nm may correspond to the debris from degradation. PVAX nanoparticles showed degradation and erosion on their surface at 1 h post-incubation with H_2O_2 (Figure 1G). These observations suggest that CO_2 gas bubbles adhere to the surface of PVAX nanoparticles and expand PVAX nanoparticles. TEM images also confirmed the bubble formation and partial degradation on the surface of PVAX nanoparticles during the incubation with H_2O_2 (Figure 1H). After 24 h of incubation with H_2O_2 , PVAX nanoparticles significantly degraded and lost structural integrity. H_2O_2 -triggered CO_2 generation of PVAX nanoparticles supports our hypothesis that PVAX nanoparticles respond to H_2O_2 , leading to CO_2 bubble

generation.

H_2O_2 -dependent echogenic properties of PVAX nanoparticles *in vitro*

We visualized the generation of CO_2 bubbles from PVAX microparticles using an optical microscope. PVAX microparticles with a mean diameter of ~ 10 μm were utilized because nanoparticles could not be observed under the optical microscope. As shown in Figure 2A, in the absence of H_2O_2 , PVAX nanoparticles swelled slightly, but maintained their structural integrity. Few bubbles were observed with PVAX nanoparticles. In contrast, after the addition of H_2O_2 (100 μM), PVAX microparticles rapidly generated a large number of CO_2 bubbles, which adhere to their surface. As the incubation time increased, the diameter of PVAX microparticles significantly increased and CO_2 bubbles also became larger due probably to expansion or coalescence of CO_2 nanobubbles into microbubbles. These observations are in good agreement with the results of DLS and TEM and suggest that PVAX nanoparticles may serve as efficient ultrasound contrast agents by scattering the ultrasound signal under the pathological conditions associated with a high level of H_2O_2 .

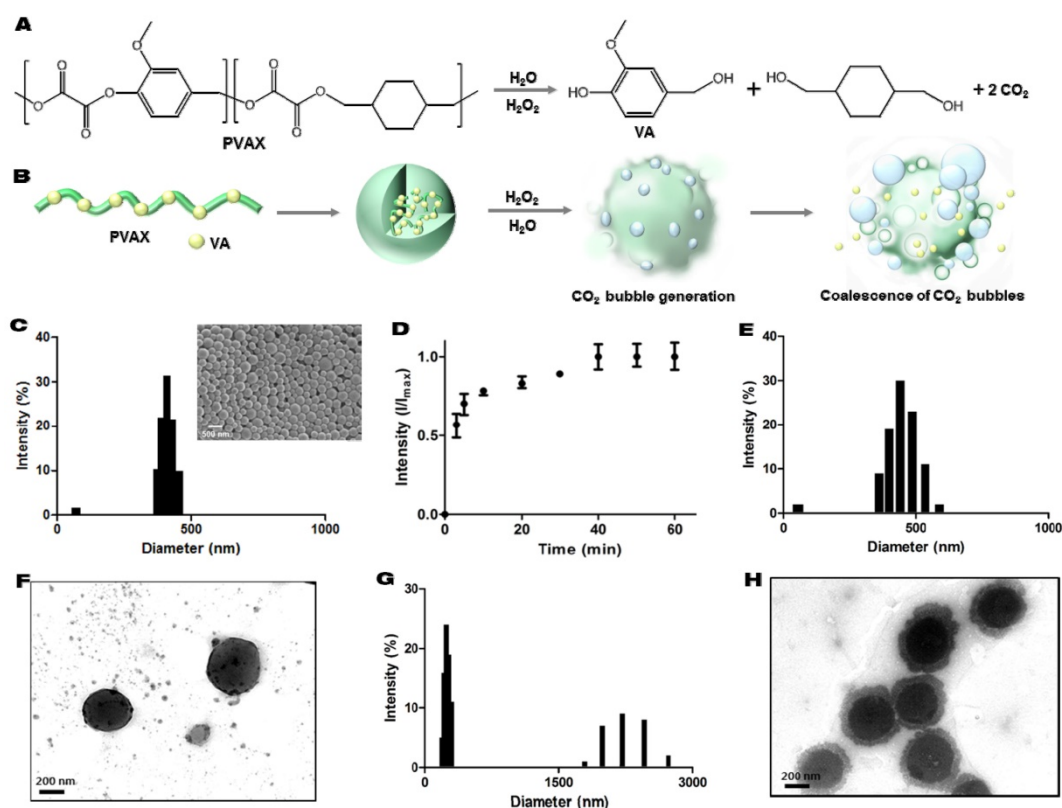


Figure 1. H_2O_2 -triggered CO_2 bubble-generating PVAX nanoparticles as an ultrasound contrast agent. (A) Chemical structure of PVAX and H_2O_2 -triggered degradation for CO_2 generation. (B) A schematic diagram of H_2O_2 -triggered CO_2 bubble generation by PVAX nanoparticles. (C) Particles size distribution of PVAX nanoparticles by dynamic light scattering. The inset is a representative scanning electron micrograph of PVAX nanoparticles. (D) Time-dependent CO_2 generation by PVAX nanoparticles in the presence of H_2O_2 . Values are mean \pm s.d. (n=4). (E) Particles size distribution of PVAX nanoparticles 12 h after incubation under the aqueous condition without H_2O_2 . (F) A representative TEM image of PVAX nanoparticles before the treatment with H_2O_2 . (G) Particles size distribution of PVAX nanoparticles 12 h after incubation under the aqueous condition with 100 μM of H_2O_2 . (H) A representative TEM image of PVAX nanoparticles after 1 h incubation with H_2O_2 .

In order to investigate the echogenic properties of PVAX nanoparticles, agarose gel phantom tests were performed with various concentrations of H₂O₂ at room temperature. Under aqueous conditions without H₂O₂, PVAX nanoparticles showed negligible echogenicity under the ultrasound field for 120 min of observation, because PVAX nanoparticles could not generate echogenic bubbles (Figure 2B). In the presence of H₂O₂ at concentrations more than 50 μM, however, PVAX nanoparticles exhibited significantly increased ultrasound contrast for 60 min, indicating the continuous generation of CO₂ bubbles from H₂O₂-triggered oxidation of PVAX.

The ultrasound signal intensity of PVAX nanoparticles increased proportionally with the concentration of H₂O₂, but the echo persistence decreased with increasing the concentration of H₂O₂ (Figure 2C). It can be explained by the rationale that the higher echo intensity at a higher concentration of H₂O₂ is attributed to the accelerated formation of a larger amount of CO₂ bubbles due to the faster H₂O₂-triggered oxidation of PVAX. However, the echo signal decayed faster at a higher level of H₂O₂ because PVAX nanoparticles dissociated faster to lose their structural integrity. The echogenicity of PVAX nanoparticles and its persistence were also evaluated in comparison with SonoVue as a control, which is one of most widely used ultrasound contrast agents in clinics. SonoVue, gas-filled microbubbles exhibited remarkably strong ultrasonographic signals from the

beginning of observation, but its intensity rapidly faded away due to their poor structural robustness. SonoVue showed a higher echo signal than PVAX nanoparticles at early time points. However, PVAX nanoparticles showed higher signal intensity than SonoVue at 30 min and also exhibited longer persistence than SonoVue. Taken together, H₂O₂-triggered CO₂ bubble generation is responsible for enhanced echogenicity of PVAX nanoparticles and PVAX nanoparticles may be suitable for ultrasonographic imaging of pathological conditions associated with a high level of H₂O₂.

Ultrasonographic imaging of contusion injury

To test whether the H₂O₂-triggered echogenic properties of PVAX nanoparticles translates to the *in vivo* setting, we investigated the potential of PVAX nanoparticles as ultrasound contrast agents using a rat model of contusion injury. As PVAX nanoparticles were designed to generate the echo signal in a H₂O₂-triggered manner, we first investigated the level of H₂O₂ in the contusion injury of muscles. Figure 3A illustrates the level of H₂O₂ in muscles before and 6 h after contusion injury, determined by Amplex Red assay. Injured triceps surae muscles exhibited more than 2-fold higher level of H₂O₂ compared to the non-injured tissues. These results clearly demonstrate that the level of H₂O₂ is significantly elevated during the contusion injury of muscles.

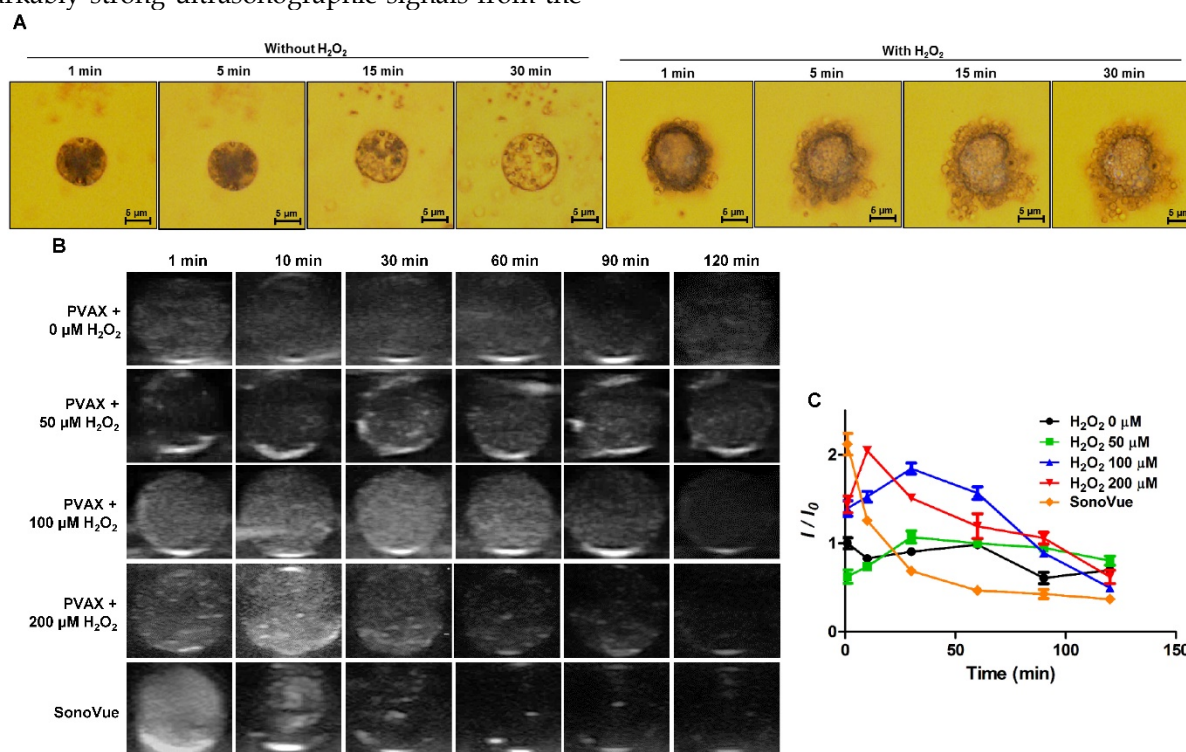


Figure 2. Time-dependent echogenic properties of PVAX nanoparticles. (A) Optical microscopic images of CO₂ bubble generating PVAX particles in the absence or presence of H₂O₂. Data are representatives of three independent experiments. (B) Ultrasound imaging of PVAX nanoparticles in the agarose gel phantom in the presence of H₂O₂. (C) Quantification of ultrasound signal intensity. PVAX nanoparticles were suspended in PBS containing various concentration of H₂O₂ at a concentration of 1 mg/mL.

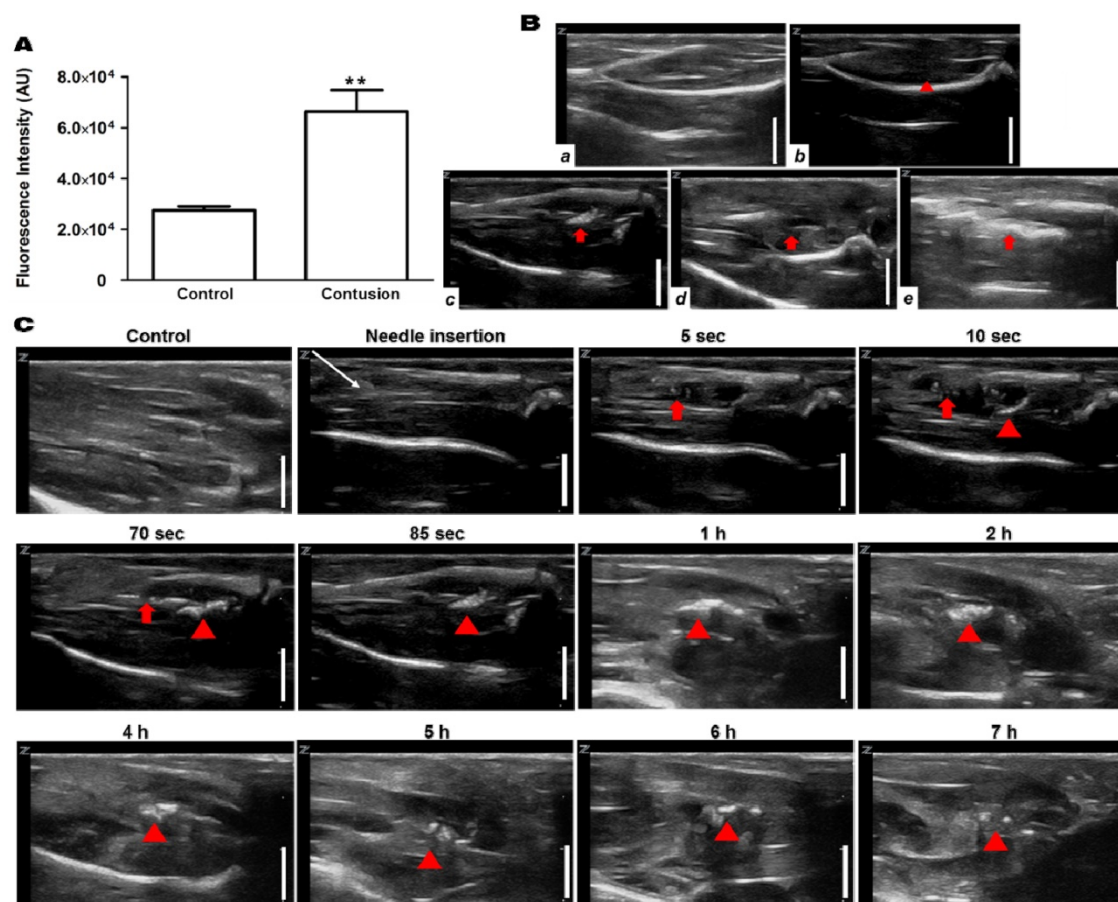


Figure 3. Ultrasonographic imaging of skeletal muscles. (A) Determination of the level of H_2O_2 in skeletal muscles before and after contusion injury. Tissues were collected at 6 h post-contusion injury and the level of H_2O_2 in tissue lysates were determined using Amplex red assay. $**p < 0.01$. Data are mean \pm s.d. ($n=4$). (B) Ultrasonography of muscles with contusion injury obtained using various ultrasound contrast agents. Ultrasonographic imaging was obtained immediately after injection of contrast agents. a) No contusion. b) Contusion only, c) Contusion + PVAX nanoparticles, d) Contusion + PLGA nanoparticles, e) Contusion + SonoVue. An arrow-head indicate the contusion site. Arrows indicate the ultrasonographic imaging effect by injectants. (C) Time courses of ultrasonography of contusion injury using PVAX nanoparticles. The syringe needle was placed into the muscles near injured site (white arrow) and PVAX nanoparticles were injected. After the injection of PVAX nanoparticles, significantly enhanced ultrasonographic contrast was observed immediately around the injected area (arrow). Then, the hyperechoic PVAX nanoparticles were observed in the injured area (arrow-head) at ~ 10 sec after injection and they exhibited remarkable contrast enhancement in the injured site. The scale bar is 5 mm. Data are representative of three independent experiments.

After the direct injection of PVAX nanoparticles into the muscles adjacent to the contusion site, ultrasonography was conducted on the injury area of the triceps surae muscles. Hyperechoic patterns in normal fibroadipose septa and muscle fascicles were observed in non-injured muscles, while injured muscles showed a slightly hypoechoic area in the muscle fascicles, corresponding to the lesion of muscle tissues (Figure 3Ba-b). After the injection of PVAX nanoparticles (300 μl of 1 mg/ml in saline), significantly enhanced ultrasonographic contrast was observed immediately in the injured area (Figure 3Bc and Figure S1). Interestingly, the hyperechoic PVAX nanoparticles were observed in the injured area from ~ 10 sec-post injection and they exhibited remarkable contrast enhancement. The significant ultrasonographic contrast enhancement was observed for ~ 4 h after the injection of PVAX nanoparticles (Figure 3C and Figure S2). The region with high echo signal could be regarded as the site of contusion injury.

In order to confirm the H_2O_2 -triggered

ultrasound contrast enhancement of PVAX nanoparticles, we prepared PLGA nanoparticles of the same size as a control because PLGA does not generate CO_2 bubbles. The same dose of PLGA nanoparticles exhibited no distinct ultrasonographic contrast in the injury site (Figure 3Bd). These results indicate that PVAX nanoparticles continuously generate CO_2 bubbles in a H_2O_2 -triggered manner to amplify the ultrasonographic contrast significantly. We also postulated that PVAX nanoparticles readily diffuse into the fibrillar texture of muscles and remain in the injury area due to their increased size when expanded by CO_2 bubbles. It was also found that gas-filled microbubbles, SonoVue exhibited a widespread pattern of highly intense echo signals, around the injection site. However, the high echo signal was not confined to the site of contusion injury (Figure 3Be). The echo signal of SonoVue was H_2O_2 -independent and disappeared at ~ 20 min after injection.

We further evaluated the diagnostic potential of

PVAX nanoparticles using a rat model of Achilles tendon injury. Contusion injury significantly (~50%) elevated the level of H₂O₂ in Achilles tendons (Figure 4A). The normal tendons exhibited thin, fine and tightly packed linear echo textures (Figure 4Ba). In a group of rats with Achilles tendon injury, the swelling of Achilles tendon was observed, but the injury had indistinct appearance (Figure 4Bb). PLGA nanoparticles directly injected into tendino-muscular junction exhibited no distinct ultrasonographic contrast in the injury site (Figure 4Bd). However, PVAX nanoparticles directly injected exhibited significantly elevated echo signal only in the injury site (Figure 4Bc and Figure S3). SonoVue also exhibited significantly enhanced ultrasonographic contrast in a widespread area surrounding the injection site (Figure 4Be), a different pattern from PVAX nanoparticles.

Anti-inflammatory effects of PVAX nanoparticles on contusion injury

To evaluate the anti-inflammatory activities of PVAX nanoparticles in the contusion injury of muscles and Achilles tendons, we investigated the mRNA expression of pro-inflammatory cytokines by RT-PCR assay at 3 days after the injection of PVAX nanoparticles (Figure 5). Contusion injury in triceps surae muscles and Achilles tendons significantly elevated the level of mRNA of iNOS, IL-1 β and TNF- α , compared to the sham. However, single injection of PVAX nanoparticles into the site of contusion injury in triceps surae muscles and Achilles tendons significantly suppressed the expression of pro-inflammatory cytokines. Therapeutic effects of PVAX nanoparticles can be explained by H₂O₂-scavenging and their intrinsic anti-inflammatory activity [27, 30].

Effects of PVAX nanoparticles on musculoskeletal apoptosis

In order to examine the anti-apoptotic activity of PVAX nanoparticles, the level of apoptosis-related proteins was determined by Western blot assay. Contusion injury in triceps surae muscles caused the significant upregulation of Bax and downregulation of Bcl-2 compared to the sham, which are typical phenotypes associated with apoptosis [31]. However, injection of PVAX nanoparticles remarkably suppressed the contusion-mediated apoptosis, evidenced by the upregulation of pro-caspase-3 and Bcl-2 and downregulation of Bax (Figure 6A and B). PVAX nanoparticles also suppressed remarkably the expression of pro-apoptotic proteins in the Achilles tendon of contusion injury (Figure 6C and D). These findings indicate that PVAX nanoparticles exert potent anti-apoptotic activities.

Histological examination

The non-injured tissues of triceps surae muscles and Achilles tendons showed characteristic normal fibrillar structure and exhibited no inflammatory cell infiltrates (Figure 7A). Intramuscular injection of PVAX nanoparticles into normal tissues caused non-significant histological damages. Contusion injury caused significant damages in the triceps surae muscles, evidenced by discontinuous irregular fibrillar texture. Contusion injury also induced massive inflammatory cell infiltration, confirmed by immunofluorescent staining with CD68 antibody (Figure 7B). Injured tissues treated with PVAX nanoparticles showed less tissue damages and less leukocyte infiltration than the contusion-only tissue. Contusion injury also significantly damaged the fibrillar textures in Achilles tendons and PVAX nanoparticles remarkably recovered the tissue damages.

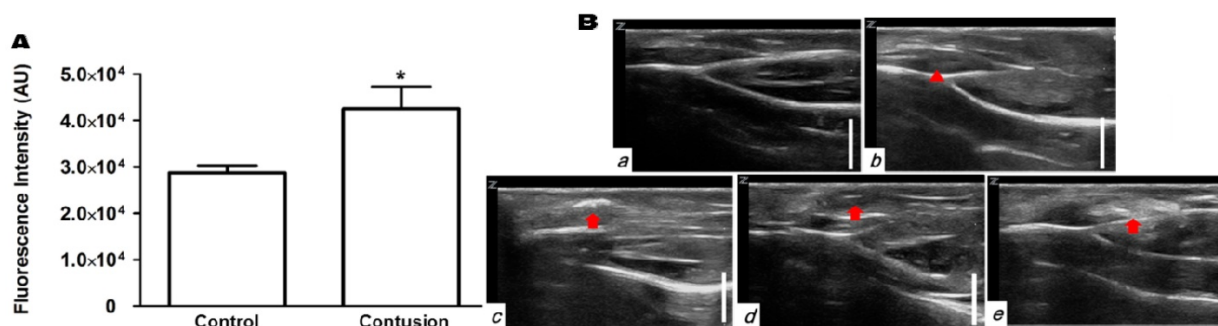


Figure 4. Ultrasonographic imaging of Achilles tendons. (A) Determination of the level of H₂O₂ in Achilles tendon before and after contusion injury. Tissues were collected at 6 h post-contusion injury and the level of H₂O₂ in tissue lysates were determined using Amplex red assay. **p*<0.05, Data are mean \pm s.d. (n=4). (B) Ultrasonographic images of contusion injury in Achilles tendon using various ultrasound contrast agents. Ultrasonographic imaging was obtained after immediately after injection of contrast agents. a) No contusion. b) Contusion only, c) Contusion + PVAX nanoparticles, d) Contusion + PLGA nanoparticles, e) Contusion + SonoVue. Arrow-heads indicate the contusion site. Arrows indicate the ultrasonographic imaging effect by injectants. Data are representative of three independent experiments. The scale bar is 5 mm.

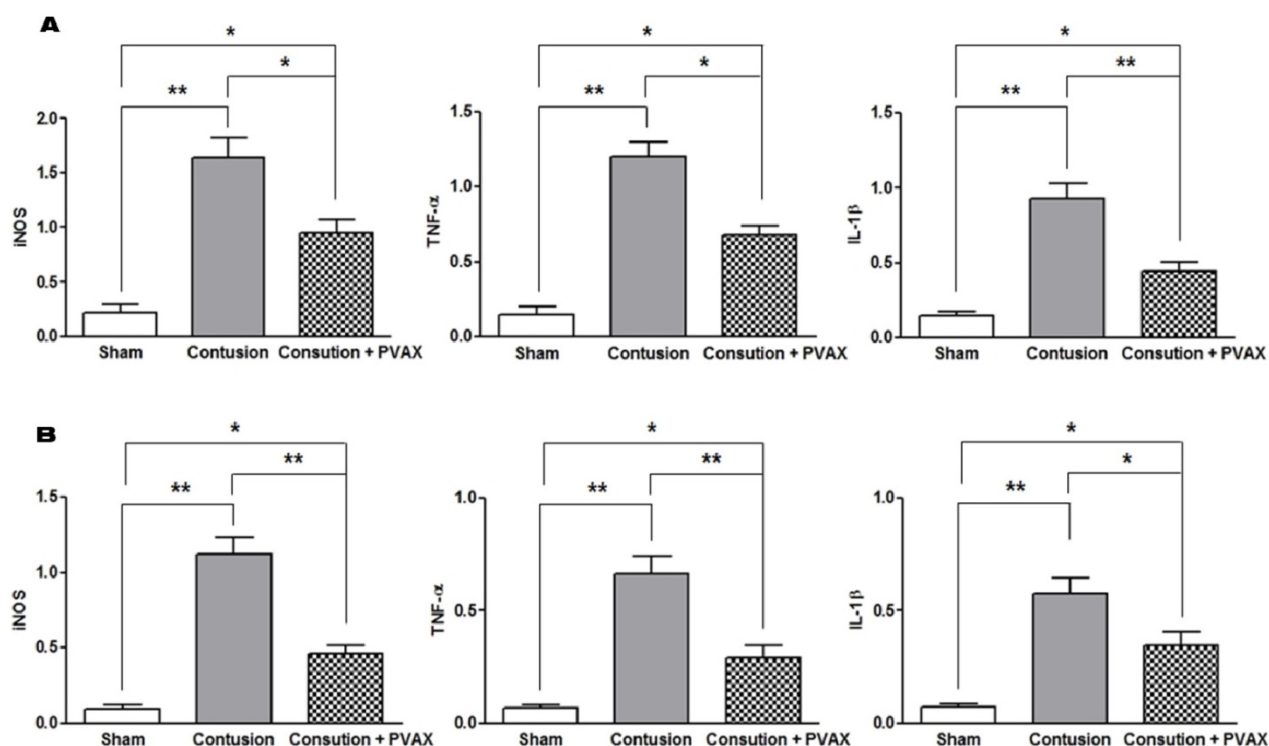


Figure 5. Anti-inflammatory activities of PVAX nanoparticles injected to the lesion of contusion injury. (A) Triceps surae muscles. (B) Achilles tendons. * $p < 0.05$, ** $p < 0.01$. Data are mean \pm s.d. (n=4). The tissues were excised at 3 days after injection of PVAX nanoparticles and the level of mRNA was determined by RT-PCR.

In order to confirm the anti-apoptotic activity of PVAX nanoparticles, we performed TUNEL staining of tissues of triceps surae muscles and Achilles tendons (Figure 8). The tissues of injured triceps surae muscles and Achilles tendons showed a number of TUNEL-positive cells, corresponding to apoptotic cells. However, injection of PVAX nanoparticles remarkably inhibited contusion-mediated apoptosis. These results are in good agreement with the results of Western blot assay (Figure 6).

Toxicity of PVAX nanoparticles

We finally performed MTT assay to investigate the cytotoxicity of PVAX nanoparticles. PVAX nanoparticles induced no or negligible reduction in the viability of RAW264.7 cells (Figure S4) after 24 h of treatment. To test the *in vivo* safety profile of PVAX, mice were intravenously administered with PVAX nanoparticles at a dose of 20 mg/kg. There was no significant histological evidence of acute toxicity in the major organs associated with administration of PVAX nanoparticles at 7 day post-administration (Figure S5), demonstrating the excellent biocompatibility of PVAX.

Discussion

Ultrasonography is one of the most widely used diagnostic modalities in clinics due to its low expense and fast real-time imaging with no radiation hazard

[10, 32-33]. In ultrasonography of musculoskeletal systems, echogenic structures correspond to normal fibroadipose septa of the perimysium surrounding hypoechoic muscle fascicles, which appear as a linear hyperechoic parallel strand. Muscle injury such as rupture is characterized by focal hypoechoic irregularity, echogenicity change and echo-free areas. While normal tendons exhibit hyperechoic fibrillar echotexture due to highly organized collagen [5-6, 33], rupture or tear of tendons appears hypoechoic with fragmented contiguous fibrils [6, 34]. However, when injury is small and mild, diagnostic usage of musculoskeletal ultrasonography is limited by operator dependency and reduced conspicuity [35-36]. Even with the recent advancement of musculoskeletal ultrasonography such as wideband Doppler imaging, spatial compound imaging, extended field of view imaging and elastographic imaging, there are still great needs to improve the diagnostic potential of ultrasonography for small musculoskeletal lesions [10, 34, 37-39]. Microbubble contrast agents have been commonly used to enhance the contrast in intravascular ultrasonography and have recently been employed for musculoskeletal ultrasonography [13-15]. In this regard, we sought to establish whether H_2O_2 -triggered bubble-generating PVAX nanoparticles could serve as ultrasound contrast agents for skeletal muscle and tendon injuries.

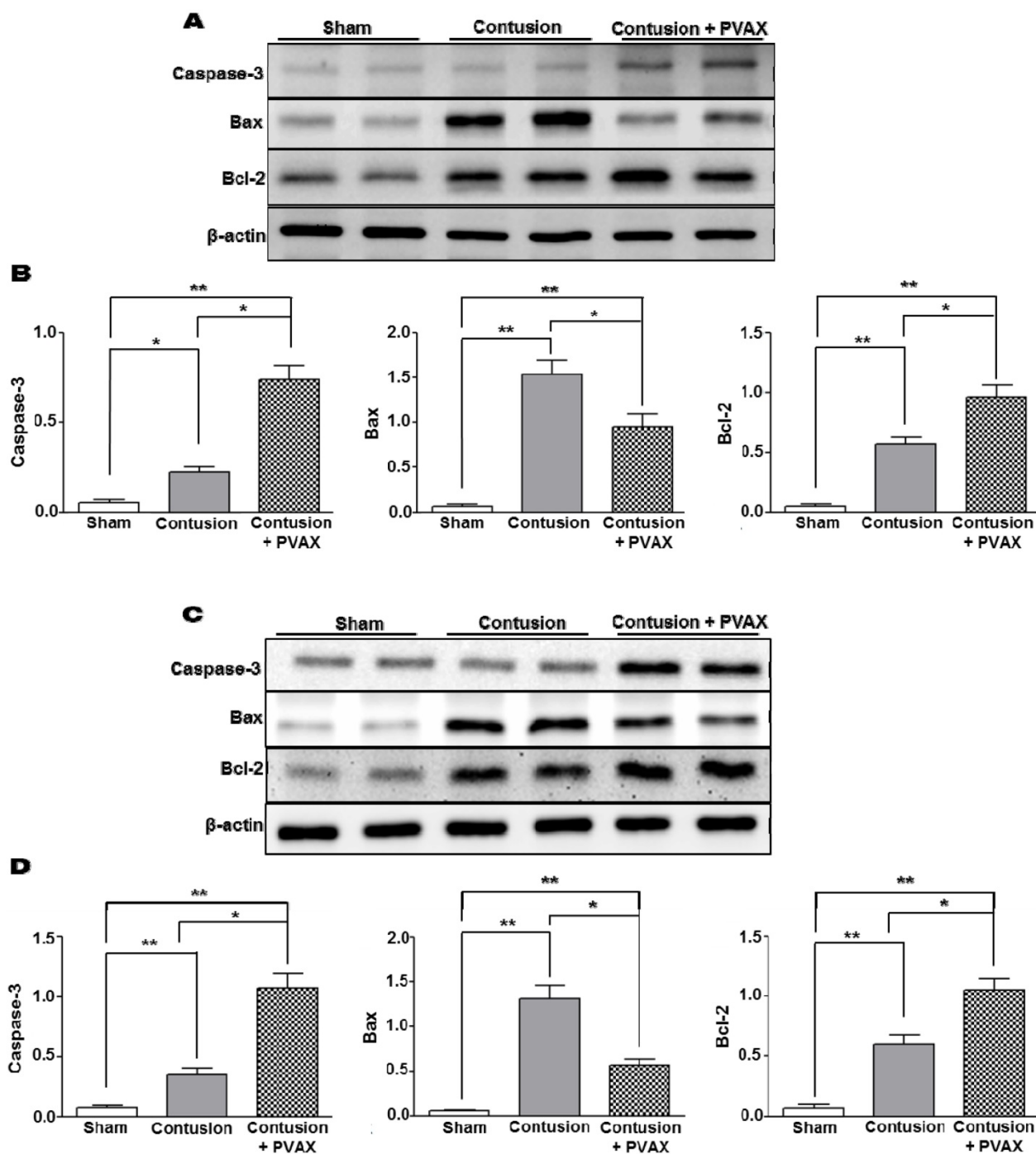


Figure 6. Anti-apoptotic activities of PVAX nanoparticles injected to the lesion of contusion injury in triceps surae muscles and Achilles tendons. (A) Effects of PVAX nanoparticles on the expression of apoptosis-related proteins in triceps surae muscles. (B) Quantification of apoptosis-related proteins in triceps surae muscles. (C) Effects of PVAX nanoparticles on the expression of apoptosis-related proteins in Achilles tendons. (D) Quantification of apoptosis-related proteins in Achilles tendons. The tissues were excised at 3 days after injection of PVAX nanoparticles. * $p < 0.05$, ** $p < 0.01$. Data are mean \pm s.d. (n=4).

In the previous studies, muscle contusion injury was induced by a metallic mass (200~204 g) falling through a guide tube from the height of 16~37 cm [40-41]. On the contrary, we used a compression instrument to induce the identical level of damage at a precise location. Contusion injury was induced by compressing hind limb muscles and Achilles tendons using a flat probe of 3 mm diameter. As we

hypothesized that PVAX nanoparticles generate CO₂ bubbles in a H₂O₂-triggered manner, we first determined the level of H₂O₂ generated during the contusion injury. Although the absolute concentration of H₂O₂ under pathological conditions could not be determined by Amplex red assay, the level of H₂O₂ was significantly elevated after contusion injury in triceps surae muscles and Achilles tendons (Figure 3A

and Figure 4A). These findings are in good accordance with the previous studies reporting that a large amounts of ROS are produced by tissue damages such as trauma, crush injuries and mechanical injuries [21-24]. The elevated level of H_2O_2 generated during the contusion injury of triceps of surae muscles and Achilles tendons seems high enough to generate CO_2 bubbles through the oxidation of peroxalate esters in PVAX, leading to ultrasound contrast enhancement (Figure 3 and 4).

Quantification of H_2O_2 *in vivo* is a great challenge due to the lack of methodology to detect H_2O_2 with high specificity and there has been controversy regarding the concentration of pathological and physiological H_2O_2 [42-43]. Although the absolute concentration of H_2O_2 is unknown, the level of H_2O_2

used in the phantom study and microscopy might be higher than its pathological level. We selected the levels of H_2O_2 based on the amount of PVAX nanoparticles required for the assay and the sensitivity limit of the assay. There are a number of previous studies, in which super-physiological levels of H_2O_2 were used to investigate the H_2O_2 -responsiveness of numerous oxidation-responsive polymers [44-46]. Even 500 mM of H_2O_2 was used to demonstrate the H_2O_2 -responsiveness of oxidation sensitive poly(phenylene sulfide) microparticles [47]. Compared to these previous studies, the level of H_2O_2 used in the present study was much lower and might be closer to its pathophysiological level.

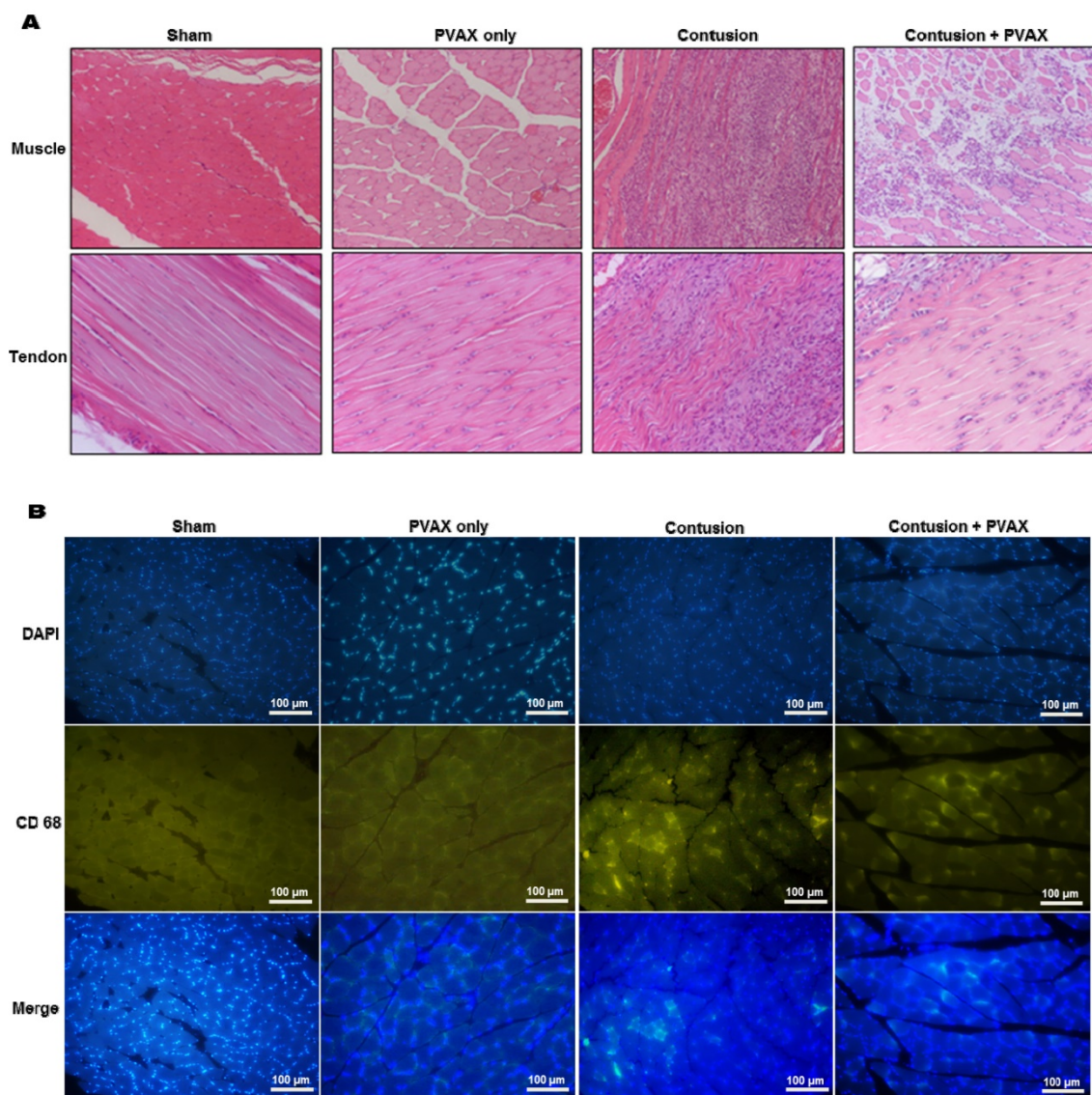


Figure 7. Histological examination of triceps surae muscles and Achilles tendons. (A) H&E staining of tissues. (B) Immunofluorescent staining with macrophage marker CD68 in muscles. The tissues were excised at 3 days after injection of PVAX nanoparticles (n=6).

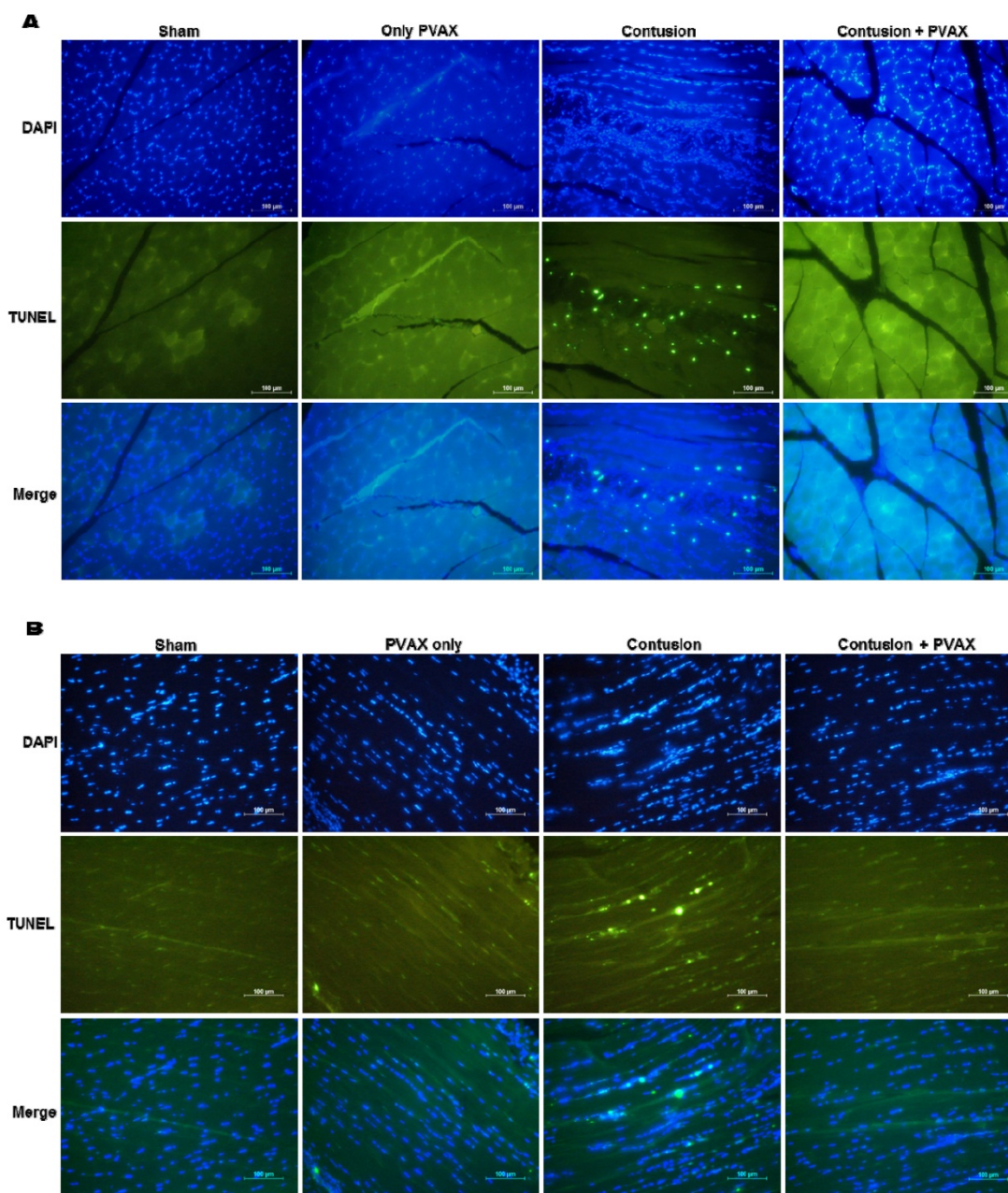


Figure 8. TUNEL staining of triceps surae muscles (A) and Achilles tendons (B). The tissues were excised at 3 days after injection of PVAX nanoparticles (n=6).

We performed preliminary studies to determine the most effective and suitable administration route for PVAX nanoparticles. After the induction of contusion injury in hind limb muscles, PVAX nanoparticles were administered intravenously and intraperitoneally. PVAX nanoparticles upon intravenous and intraperitoneal administration induced no echogenic changes in the site of contusion injury, suggesting that they could not extravasate from blood vessels to target the site of contusion injury in hind limb muscles. We therefore selected intramuscular injection to deliver PVAX nanoparticles directly to the injury site based on the notion that

ultrasonography-guided peri-musculotendinous injections are very common treatment in musculoskeletal disorders [48-49]. PVAX nanoparticles directly injected into the region adjacent to the contusion site showed considerable ultrasound contrast enhancement, with significantly different pattern from SonoVue (Figures 3 and 4). While SonoVue provided increased echogenicity in the widespread area around the lesion, PVAX nanoparticles exhibited significantly enhanced focal contrast around the lesion. H₂O₂-nonresponsive PLGA nanoparticles showed no contrast enhancement, demonstrating that echogenicity of

CO₂-bubble-generating PVAX nanoparticles is triggered by H₂O₂ overproduced in the site of contusion injury. The significantly enhanced contrast signal lasted for ~ 4 h, suggesting that PVAX nanoparticles are stable to keep their structural integrity under the pathophysiological condition for several hours.

We previously developed PVAX as a polymeric prodrug of vanillyl alcohol, which is the main ingredient of *Gastrodia elata* and is known to have potent antioxidant and anti-inflammatory effects. PVAX was designed to scavenge H₂O₂ through H₂O₂-mediated oxidation of peroxalate ester and then release vanillyl alcohol to display antioxidant and anti-inflammatory actions [27-28]. Our previous studies reported that PVAX nanoparticles inhibit apoptosis and inflammation in mouse models of hind limb ischemia/reperfusion injury and acute liver failure. The present study also clearly demonstrates that PVAX nanoparticles exert highly potent anti-inflammatory activity in contusion injury by suppressing macrophage recruitment and inhibiting the expression of pro-inflammatory TNF- α , iNOS and IL-1 β . PVAX nanoparticles also remarkably inhibited apoptosis, evidenced by TUNEL staining and Western blotting of caspase-3, Bcl-2 and Bax.

Theranostics refers to the combination of disease diagnosis and therapy [10]. With the rapid advancement of nanotechnology, theranostic nanomedicine has been emerging as a promising therapeutic paradigm. Microbubbles can also be used for more than diagnosis. Several lines of studies using various animal models report that microbubbles loaded with plasmid DNA or drugs hold great potential as a theranostic agent, given their propensity to be visualized under physiological conditions and their ability to facilitate drug delivery [10, 50]. In the present study, we investigated the potential of H₂O₂-triggered bubble-generating PVAX nanoparticles as nano-theranostic agents for musculoskeletal injuries. Unlike drug-loaded microbubbles, PVAX nanoparticles themselves could exhibit high potent intrinsic anti-inflammatory and anti-apoptotic activities, which are enough to exert beneficial therapeutic effects in contusion injury. PVAX nanoparticles could also specifically detect the contusion injury in a H₂O₂-triggered manner, which is their appealing feature in ultrasonography. To our best understanding, we report, for the first time, the H₂O₂-triggered bubble generating theranostic nanoparticles for ultrasonography and therapy of musculoskeletal injury. Intramuscular injection of drugs has been commonly used in clinics [48-49, 51]. For example, peri-musculotendinous corticosteroid injection has been widely performed to patients with

hamstring tendinopathy [52]. Therefore, we anticipate that if PVAX nanoparticles are loaded with drugs, their therapeutic efficacy could be remarkably enhanced while keeping their potential as H₂O₂-sensitive ultrasound contrast agents.

In musculoskeletal ultrasonography, the operator should be well-trained in the techniques and have detailed understanding of musculoskeletal anatomy and sufficient experience of examining normal and abnormal muscle tissues in the static and dynamic state. Even ultrasonographic experts have difficulties to find right diagnosis when the lesion is minor and tiny. Therefore, H₂O₂-responsive bubble-generating PVAX nanoparticles would help examiners find the right diagnosis of mild and tiny musculoskeletal injuries. Although the results of this proof-of-principle study demonstrate the tremendous potential of PVAX nanoparticles as theranostic agents for musculoskeletal injury, the limitation of the present study is that translational potential of PVAX nanoparticles as a nano-theranostic agent was evaluated only for acute injuries. Further studies using various animal models such as subacute and chronic injuries are warranted to maximize the clinical potential in future.

Conclusions

We evaluated the potential of H₂O₂-triggered bubble-generating anti-inflammatory PVAX nanoparticles as nano-theranostic agents for musculoskeletal injuries using a rat model of musculoskeletal contusion injury. PVAX nanoparticles administrated through intramuscular and peri-tendinous injection into the lesions of mechanical injury significantly enhanced the ultrasonographic contrast and exerted remarkable anti-inflammatory and anti-apoptotic effects. These findings suggest that H₂O₂-triggered bubble-generating PVAX nanoparticles have tremendous potential as ultrasound contrast agents and therapeutic agents for various musculoskeletal diseases.

Supplementary Material

Supplementary figures.

<http://www.thno.org/v07p2463s1.pdf>

Acknowledgements

This work was supported by a grant of Korea Health Technology R&D Project through the Korea Health Industry Development Institute funded by the Ministry of Health & Welfare (HI13C1370 and HI15C1529) and the Technology Innovation Program (10052749) funded by Ministry of Trade, Industry and Energy, Republic of Korea.

Competing Interests

The authors have declared that no competing interest exists.

References

- Rantanen J, Thorsson O, Wollmer P, Hurme T, Kalimo H. Effects of therapeutic ultrasound on the regeneration of skeletal myofibers after experimental muscle injury. *Am J Sports Med.* 1999; 27: 54-9.
- Kannus P. Etiology and pathophysiology of chronic tendon disorders in sports. *Scand J Med Sci Sports.* 1997; 7: 78-85.
- Kallinen M, Markku A. Aging, physical activity and sports injuries. *Sports Med.* 1995; 20: 41-52.
- Fejer R, Ruhe A. What is the prevalence of musculoskeletal problems in the elderly population in developed countries? A systematic critical literature review. *Chiropr Man Therap.* 2012; 20: 31-.
- Min HS, Son S, Lee TW, Koo H, Yoon HY, Na JH, Choi Y, Park JH, Lee J, Han MH, Park R-W, Kim I-S, Jeong SY, Rhee K, Kim SH, Kwon IC, Kim K. Liver-Specific and Echogenic Hyaluronic Acid Nanoparticles Facilitating Liver Cancer Discrimination. *Adv Funct Mater.* 2013; 23: 5518-29.
- Zamorani M, Valle M. Muscle and Tendon. In: Bianchi, S.; Martinoli, C. ed. *Ultrasound of the Musculoskeletal System*, Berlin: Springer Berlin Heidelberg, 2007: 45-96.
- Jacobson JA. Musculoskeletal Ultrasound: Focused Impact on MRI. *Am J Roentgenol.* 2009; 193: 619-27.
- Lento PH, Strakowski JA. The Use of Ultrasound in Guiding Musculoskeletal Interventional Procedures. *Phys Med Rehabil Clin N Am.* 2010; 21: 559-83.
- Joines MM, Motamedi K, Seeger LL, DiFiori JP. Musculoskeletal interventional ultrasound. *Semin Musculoskelet Radiol.* 2007; 11: 192-8.
- Kiessling F, Fokong S, Koczera P, Lederle W, Lammers T. Ultrasound Microbubbles for Molecular Diagnosis, Therapy, and Theranostics. *J Nucl Med.* 2012; 53: 345-8.
- Son S, Min HS, You DG, Kim BS, Kwon IC. Echogenic nanoparticles for ultrasound technologies: Evolution from diagnostic imaging modality to multimodal theranostic agent. *Nano Today.* 2014; 9: 525-40.
- Postema M, Gilja OH. Contrast-enhanced and targeted ultrasound. *World J Gastroenterol.* 2011; 17: 28.
- Lv F, Tang J, Luo Y, Ban Y, Wu R, Tian J, Yu T, Xie X, Li T. Contrast-enhanced ultrasound assessment of muscle blood perfusion of extremities that underwent crush injury: an animal experiment. *J Trauma Acute Care Surg.* 2013; 74: 214-9.
- Chang K-V, Lew HL, Wang T-G, Chen W-S. Use of contrast-enhanced ultrasonography in musculoskeletal medicine. *Am J Phys Med Rehabil.* 2012; 91: 449-57.
- Stramare R, Raffener B, Ciprian L, Scagliori E, Coran A, Perissinotto E, Fiocco U, Beltrame V, Rubaltelli L. Evaluation of finger joint synovial vascularity in patients with rheumatoid arthritis using contrast-enhanced ultrasound with water immersion and a stabilized probe. *J Clin Ultrasound.* 2012; 40: 147-54.
- Foroutan F, Jokerst JV, Gambhir SS, Vermesh O, Kim H-W, Knowles JC. Sol-Gel Synthesis and Electrospinning of Biodegradable (P2O5)(55)-(CaO)(30)-(Na2O)(15) Glass Nanospheres as a Transient Contrast Agent for Ultrasound Stem Cell Imaging. *ACS Nano.* 2015; 9: 1868-77.
- Min HS, Kang E, Koo H, Lee J, Kim K, Park R-W, Kim I-S, Choi Y, Kwon IC, Han M. Gas-generating polymeric microspheres for long-term and continuous in vivo ultrasound imaging. *Biomaterials.* 2012; 33: 936-44.
- Kang E, Min HS, Lee J, Han MH, Ahn HJ, Yoon I-C, Choi K, Kim K, Park K, Kwon IC. Nanobubbles from Gas-Generating Polymeric Nanoparticles: Ultrasound Imaging of Living Subjects. *Angew Chem Int Ed.* 2010; 49: 524-8.
- Min KH, Min HS, Lee HJ, Park DJ, Yhee JY, Kim K, Kwon IC, Jeong SY, Silvestre OF, Chen X, Hwang Y-S, Kim E-C, Lee SC. pH-Controlled Gas-Generating Mineralized Nanoparticles: A Theranostic Agent for Ultrasound Imaging and Therapy of Cancers. *ACS Nano.* 2015; 9: 134-45.
- Kang C, Cho W, Park M, Kim J, Park S, Shin D, Song C, Lee D. H2O2-triggered bubble generating antioxidant polymeric nanoparticles as ischemia/reperfusion targeted nanotheranostics. *Biomaterials.* 2016; 85: 195-203.
- Kerkweg U, Petrat F, Korth H-G, de Groot H. Disruption of skeletal myocytes initiates superoxide release: contribution of NAD (P) H oxidase. *Shock.* 2007; 27: 552-8.
- Filippin LI, Moreira AJ, Marroni NP, Xavier RM. Nitric oxide and repair of skeletal muscle injury. *Nitric Oxide.* 2009; 21: 157-63.
- Bestwick C, Maffulli N. Reactive oxygen species and tendinopathy: do they matter? *Br J Sports Med.* 2004; 38: 672-4.
- Bestwick CS, Maffulli N. Reactive Oxygen Species and Tendon Problems: Review and Hypothesis. *Sports Med Arthro Review.* 2000; 8: 6-16.
- Close GL, Ashton T, McArdle A, Maclaren DP. The emerging role of free radicals in delayed onset muscle soreness and contraction-induced muscle injury. *Comp Biochem Physiol A: Mol Integr Physiol.* 2005; 142: 257-66.
- Barbieri E, Sestili P. Reactive Oxygen Species in Skeletal Muscle Signaling. *J Signal Transduct.* 2012; 2012: 1-17.
- Lee D, Bae S, Hong D, Lim H, Yoon JH, Hwang O, Park S, Ke Q, Khang G, Kang PM. H2O2-responsive molecularly engineered polymer nanoparticles as ischemia/reperfusion-targeted nanotherapeutic agents. *Sci Rep.* 2013; 3: 1-8.
- Park S, Yoon J, Bae S, Park M, Kang C, Ke Q, Lee D, Kang PM. Therapeutic use of H₂O₂-responsive anti-oxidant polymer nanoparticles for doxorubicin-induced cardiomyopathy. *Biomaterials.* 2014; 35: 5944-53.
- Jeong D, Kang C, Jung E, Yoo D, Wu D, Lee D. Porous antioxidant polymer microparticles as therapeutic systems for the airway inflammatory diseases. *J Control Release.* 2016; 233: 72-80.
- Ko E, Jeong D, Kim J, Park S, Khang G, Lee D. Antioxidant polymeric prodrug microparticles as a therapeutic system for acute liver failure. *Biomaterials.* 2014; 35: 3895-902.
- Stratos I, Li Z, Rotter R, Herlyn P, Mittlmeier T, Vollmar B. Inhibition of caspase mediated apoptosis restores muscle function after crush injury in rat skeletal muscle. *Apoptosis.* 2012; 17: 269-77.
- Chew K, Stevens KJ, Wang T-G, Fredericson M, Lew HL. Introduction to diagnostic musculoskeletal ultrasound - Part 2: Examination of the lower limb. *Am J Phys Med Rehabil.* 2008; 87: 238-48.
- Lew HL, Chen CPC, Wang T-G, Chew KTL. Introduction to musculoskeletal diagnostic ultrasound - Examination of the upper limb. *Am J Phys Med Rehabil.* 2007; 86: 310-21.
- Torriani M, Kattapuram SV. Musculoskeletal Ultrasound: An Alternative Imaging Modality for Sports-Related Injuries. *Top Magn Reson Imaging.* 2003; 14: 103-11.
- Barberie JE, Wong A, Cooperberg P, Carson B. Extended field-of-view sonography in musculoskeletal disorders. *Am J Roentgenol.* 1998; 171: 751-7.
- Hayashi D, Hamilton B, Guermazi A, de Villiers R, Crema MD, Roemer FW. Traumatic injuries of thigh and calf muscles in athletes: role and clinical relevance of MR imaging and ultrasound. *Insights Imaging.* 2012; 3: 591-601.
- Lin DC, Nazarian LN, O'Kane PL, McShane JM, Parker L, Merritt CR. Advantages of real-time spatial compound sonography of the musculoskeletal system versus conventional sonography. *Am J Roentgenol.* 2002; 179: 1629-31.
- Lin EC, Middleton WD, Teefey SA. Extended field of view sonography in musculoskeletal imaging. *JUltrason Med.* 1999; 18: 147-52.
- Drakonaki EE, Allen GM, Wilson DJ. Ultrasound elastography for musculoskeletal applications. *Br J Radiol.* 2012; 85: 1435-45.
- Minamoto V, Bunho S, Salvini T. Regenerated rat skeletal muscle after perimodic contusions. *Braz J Med Biol Res.* 2001; 34: 1447-52.
- Balisardo Minamoto V, Roberto Grazziano C, De Fátima Salvini T. Effect of single and periodic contusion on the rat soleus muscle at different stages of regeneration. *Anat Rec.* 1999; 254: 281-7.
- Lee D, Khaja S, Velasquez-Castano JC, Dasari M, Sun C, Petros J, Taylor WR, Murthy N. In vivo imaging of hydrogen peroxide with chemiluminescent nanoparticles. *Nat Mater.* 2007; 6: 765-9.
- Halliwell B, Clement MV, Long LH. Hydrogen peroxide in the human body. *FEBS Lett.* 2000; 486: 10-3.
- Lux CD, Joshi-Barr S, Nguyen T, Mahmoud E, Schopf E, Fomina N, Almutairi A. Biocompatible Polymeric Nanoparticles Degrade and Release Cargo in Response to Biologically Relevant Levels of Hydrogen Peroxide. *J Am Chem Soc.* 2012; 134: 15758-64.
- Mahmoud EA, Sankaranarayanan J, Morachis JM, Kim G, Almutairi A. Inflammation Responsive Logic Gate Nanoparticles for the Delivery of Proteins. *Bioconjug Chem.* 2011; 22: 1416-21.
- Song CC, Ji R, Du FS, Liang DH, Li ZC. Oxidation-Accelerated Hydrolysis of the Ortho Ester-Containing Acid-Labile Polymers. *ACS Macro Letters.* 2013; 2: 273-7.
- Poole KM, Nelson CE, Joshi RV, Martin JR, Gupta MK, Haws SLC, Kavanaugh TE, Skala MC, Duvall CL. ROS-responsive microspheres for on demand antioxidant therapy in a model of diabetic peripheral arterial disease. *Biomaterials.* 2015; 41: 166-75.
- Sofka CM, Collins AJ, Adler RS. Use of ultrasonographic guidance in interventional musculoskeletal procedures - A review from a single institution. *J Ultrason Med.* 2001; 20: 21-6.
- Coombes BK, Bisset L, Vicenzino B. Efficacy and safety of corticosteroid injections and other injections for management of tendinopathy: a systematic review of randomised controlled trials. *Lancet.* 2010; 376: 1751-67.
- Phillips LC, Dhanaliwala AH, Klibanov AL, Hossack JA, Wamhoff BR. Focused Ultrasound-Mediated Drug Delivery From Microbubbles Reduces Drug Dose Necessary for Therapeutic Effect on Neointima Formation-Brief Report. *Arterioscler Thromb Vasc Biol.* 2011; 31: 2853-5.
- Nepple JJ, Matava MJ. Soft Tissue Injections in the Athlete. *Sports Health.* 2009; 1: 396-404.
- Zissen MH, Wallace G, Stevens KJ, Fredericson M, Beaulieu CF. High Hamstring Tendinopathy: MRI and Ultrasound Imaging and Therapeutic Efficacy of Percutaneous Corticosteroid Injection. *Am J Roentgenol.* 2010; 195: 993-8.